Available online at www.sciencedirect.com

ScienceDirect

journal homepage: http://www.elsevier.com/locate/rpor

Original research article

Assessment and evaluation of MV image guidance system performance in radiotherapy

Nithya Kanakavelu[a,b,c,*], E. James Jebaseelan Samuel[b,d]

[a] Department of Radiation Oncology, Medwin Cancer Center, Hyderabad, India
[b] Photonics, Nuclear and Medical Physics Division, VIT University, Vellore, India

ARTICLE INFO

Article history:
Received 22 May 2014
Received in revised form
19 August 2014
Accepted 15 January 2015

Keywords:
Image guidance system
Quality assurance
Megavoltage imaging

ABSTRACT

Background and aim: The clinical use of imaging system in image guided radiotherapy (IGRT) necessitates performing periodic quality assurance of the system to be confident in applying corrections for patient set-up errors. We aim to develop and implement a quality assurance (QA) programme for megavoltage (MV) based image guidance system and assess its long term performance for a period of 3 years.

Materials and methods: Periodic QA tests were performed for the MV planar and cone beam computed tomography (CBCT) imaging system to assess the system safety, mechanical and geometrical accuracy, image quality and dose. The tests were performed using the equipment supplied by the manufacturer along with the image guidance system and using simple methods developed in-house. The test results were compared with expected or baseline values established during commissioning.

Results: The safety system was found to be functional. The results of mechanical and geometrical tests were in good agreement with the expected results. The system mechanical positioning was stable and reproducible within ±2 mm accuracy. The image quality and the imaging dose of the planar and CBCT imaging were found to agree with the baseline values and the manufacturer specifications.

Discussion: Throughout the three-year period, all the QA tests were within the specification. The mechanical and geometrical tests are most crucial as they directly affect the patient positioning accuracy.

Conclusion: We conclude that the MV image guidance system is efficient to perform IGRT and insist to perform periodic QA tests and calibration for the system.

* *Corresponding author*. Present address: Photonics, Nuclear and Medical Physics Division, VIT University, Vellore 632 014, India. Tel.: +91 9618015142.
E-mail address: nithya8483@gmail.com (N. Kanakavelu).
[c] Address: Department of Radiation Oncology, Medwin Cancer Center, Hyderabad 500 001, India.
[d] Address: Photonics, Nuclear and Medical Physics Division, VIT University, Vellore 632 014, India. Tel.: +91 0416 2202125.

http://dx.doi.org/10.1016/j.rpor.2015.01.002
1507-1367/

1. Background and aim

With the advances in in-room imaging system, image guided treatment has become routine in radiotherapy centres. Image guided radiotherapy (IGRT) offers benefits in monitoring the patient treatment positional accuracy, set-up uncertainties and inter-fraction anatomy changes.[1–4] The clinical use of the image guidance system necessitates implementing a quality assurance (QA) programme to monitor and maintain its performance characteristics. Several guidelines have been published for the QA programme to verify the safety, functionality and quality of the imaging system.[5–7] In our centre, safe and accurate patient positioning is our requirement to achieve with the image guidance (IG) system. Thus, the IG system safety, mechanical and geometrical accuracy, image quality and imaging dose to patient need to be assessed periodically. Therefore we implemented a QA programme to evaluate all these criteria. In this work, we share our experience in developing and implementing the QA programme for a long term of 3 years for image guidance system based on manufacturer provided test methods[8] and published guidelines.

2. Materials and methods

2.1. Medical linear accelerator and imaging system

The Medical high energy linear accelerator, Siemens Oncor Expression™ equipped with the imaging guidance (IG) system, (OPTIVUE 1000ST™, Siemens Medical solutions Inc., Concord, CA) used for megavoltage planar and cone beam computed tomography (MV CBCT) imaging, is attached to the gantry at the counter-part of the head of the linear accelerator, as shown in Fig. 1. The IG system consists of flat panel detectors which have sensors of amorphous silicon (a-Si) photo diodes that are deposited on a glass substrate with a scintillator coating. The pixels have a pitch of 400 μm and there are 1024 × 1024 pixels covering a 40 × 40 cm^2 area. The entire imaging system operates under SYNGO™ based COHERENCE™ therapist workspace which communicates with the control console, the linear accelerator, and a local patient database. The workspace contains applications allowing the automatic acquisition of projection images, image reconstruction, CT-to-CBCT image registration, and couch position adjustment. Each projection of the CBCT acquisition is corrected for defective pixels, as well as for pixel-to-pixel offset and gain variations before 3D reconstruction. The imager uses 6 MV low dose rate 50 MU/min beam to acquire MV planar images. MV CBCT images are acquired in a cone beam mode, where the 6 MV, low dose rate beam is rotated 200° from 270° to 110° and 200 projection images are acquired on the flat panel in 1° steps. The cone beam has lower dose per radiation pulse and higher radiation pulse repetition frequency when compared to regular 6 MV treatment beam. The IG system imager calibration, image acquisition, reconstruction procedure and clinical use are mentioned elsewhere.[1,8–11]

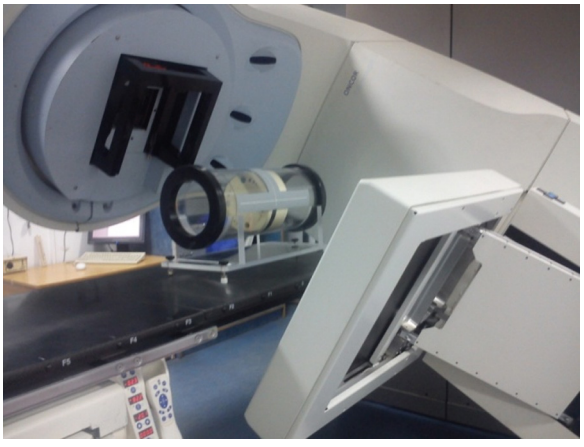

Fig. 1 – The Siemens Oncor Expression linear accelerator equipped with OPTIVUE imaging system.

2.2. Equipment for QA

X-ray reticule: The X-ray reticule (named 'X-RETIC') consists of two orthogonal radio-opaque tungsten wires, shown in Fig. 2, which can be inserted in an accessory slot in the gantry head. It is calibrated such that the intersection of the two wires corresponds exactly to the mechanical isocentre and is used to align the phantoms at the isocentre and to determine the coincidence between the accelerator isocentre and the imaging centre of the flat panel imager.

QC 3V phantom: The QC-3V phantom (Standard Imaging, Inc. USA), as shown in Fig. 2, consists of a series of bar patterns, used for measuring spatial resolution and contrast-to-noise ratio. Four large numbers engraved in the corners provide a crude visual feedback but are not used for analysis. Lines are inscribed on the front and sides for easy alignment with field lights and lasers. Planar images are acquired with the flat panel imager and analysed with the portal image processing programme.

Image quality phantom: The image quality phantom (Siemens Medical Solutions, Concord, CA), as shown in Fig. 2, is a cylindrical acrylic shell of diameter 20 cm with four solid water sections positioned axially within the shell. Section 1 is purely made of solid water of thickness 4 cm without any inserts and used to check image uniformity, noise and artefacts. Sections 2 and 4 consists of 5 circular inserts of 8 different density materials with diameter 2, 1, 0.7, 0.5 and 0.3 cm used to check low and high contrast resolution. Section 3 contains 11 bar groups and each bar group contains 5 air bars to evaluate spatial resolution. The sections 2, 3, and 4 are of thickness 2 cm each. In the outer shell, three axial planes (at the centre, head and foot of the phantom) have four tungsten beads arranged at 12, 3, 6 and 9 o'clock positions to determine the geometric positional accuracy of the CBCT image.

2.3. Imaging system QA programme

To assess and evaluate the performance of the imaging system, a periodic quality assurance programme was developed. The QA tests, frequencies and tolerances are given in Table 1. In this study, these tests were performed for a period of 3 years and the results were evaluated for its accuracy and consistency. The baseline values of these tests were defined

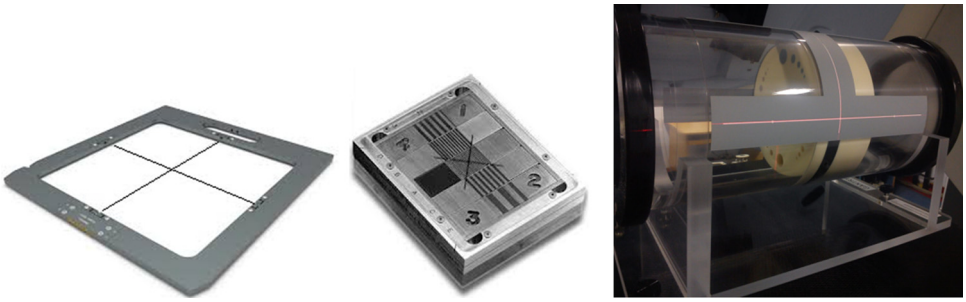

Fig. 2 – Equipment for QA: X-RETIC (left), QC 3V phantom (middle), image quality phantom (right).

during the acceptance testing and commissioning of the MV imager.

2.4. *Safety interlock checks*

Collision sensors are provided between the flat panel detector and outer cover. A safety interlock is triggered when a slight pressure is applied on the outer cover. The interlock was checked by applying a slight pressure with hands on any of the four corners of the flat panel cover and verifying the activation of the motion stop interlock which restricts all the mechanical movements of the machine. With the motion stop interlock activated, restriction of gantry, couch and imager mechanical movements were verified. The functionality of the door interlock was verified by introducing an object between the door sensors during image acquisition, which should turn off the beam.

2.5. *Mechanical and geometric accuracy tests*

Imager positioning/repositioning: The imager positioning accuracy and reproducibility are significant in the patient treatment position verification. A graph sheet was fixed over a 1 cm thick $30 \times 30\,cm^2$ slab phantom and its centre aligned with the treatment isocentre. Five radio-opaque markers were placed at known distances on the graph sheet with one marker at the centre and the other four at the four corners of a $10 \times 10\,cm^2$ area. A planar image was acquired with $15 \times 15\,cm^2$ field size, gantry angle of 0° and imager positioned at the source to imager distance (SID) of 145 cm. Then, the imager was retracted, repositioned at the same SID and imaged again. The distance between the markers was measured with the measurement tool (ruler) available in the 'Coherence Therapist' system workspace. The actual distances of the 5 markers from the isocentre were compared with the measured distance in the MV images acquired initially and after repositioning the imager.

Imaging and treatment co-ordinate coincidence: The accuracy of patient position also depends on the precision with which the imaging co-ordinate axis is aligned to the treatment co-ordinate axis. Even though the physical position of the imager is exactly set with respect to the mechanical isocentre of the machine, residual misalignment must also be accounted. The X-RETIC, as described in Section 2.2, was inserted in the machine accessory slot. A series of MV planar images were taken at four cardinal gantry angles 0°, 90°, 180° and 270° at SID 145 cm. The position of the projected X-RETIC wires represents the treatment co-ordinate axis, while the imaging co-ordinate axis can be graphically visualised in the Coherence therapist system using a 'grid display' option. The misalignment between the two axes at four gantry positions was measured with the measurement tool available in the system workspace.

Image scaling: The same set-up used for imaging positioning/repositioning was used to evaluate the scaling accuracy. MV images were acquired at different SID such as 115, 125, 135, 145, 150 and 160 cm. As all the radio-opaque markers were at known distances from each other, the acquired MV images were checked for corresponding distances between the markers.

Mechanical alignment through full range of imager travel: The MV flat panel imager can be moved vertically along the beam axis with SID between 115 and 160 cm. Throughout this range, the alignment of the imager with the mechanical isocentre was verified. With the imager at calibration SID of 145 cm, a graph sheet was fixed on the imager and the centre of X-RETIC projection was marked on it. The flat panel was moved through a range of SIDs 115, 125, 135, 145, 150, 160 cm and at each position the lateral, longitudinal shifts in the marked position from X-RETIC projection were measured. Also at each

Table 1 – QA tests for image guidance system.

Frequency	QA test	Tolerance
Daily	Safety checks	Functional
	Imager positioning/repositioning	±1 mm
	Imaging and treatment co-ordinate coincidence (single gantry angle)	±1 mm
Monthly	Imaging and treatment co-ordinate coincidence (4 cardinal gantry angles)	±1 mm
	Image scaling	±2 mm
	Mechanical alignment – full range of travel	±2 mm
	Geometric accuracy for CBCT	±2 mm
	Automatic image registration and offset calculation accuracy	±2 mm
	Image quality – planar and CBCT	Baseline ± 5%
Annual	Imaging dose	Baseline ± 3%

SID, the vertical distance between the flat panel cover and isocentre was measured, using a measuring tape.

Geometric accuracy for CBCT: The tungsten beads at the centre, head and foot of the image quality phantom, as described under Section 2.2 was used to verify geometric positional accuracy for CBCT images. MV CBCT images were acquired with the phantom aligned at the machine isocentre. In the Adaptive targeting application of Coherence workspace, the reference point cursor was placed at the centre of each bead in the CBCT image to read the three dimensional co-ordinate of each bead position and compared with the actual known position of each bead.

Automatic image registration and offset calculation accuracy: The Adaptive Targeting application of Coherence Therapist system automatically registers planning CT image data set with the acquired CBCT image data set based on mutual information algorithm. On acceptance of image registration, the software displays the table offset for correction. Its accuracy was checked by introducing a known off-set between the two datasets. Image quality phantom was scanned on a CT simulator, a simple plan was made in a treatment planning system (TPS) with planning isocentre coinciding with the centre of the phantom and the planning CT data set was exported to the Coherence workstation. The phantom was set-up with the planned isocentre coinciding with the machine isocentre. CBCT images were acquired and the system started automatic registration of acquired CBCT images and the planning CT images. The registration was visually verified in the axial, coronal and sagittal views and, when accepted, the system calculated and displayed the offset in the lateral, longitudinal and vertical directions. The CBCT scans were repeated for different known shifts introduced to the CBCT images by shifting the table in the lateral, longitudinal and vertical directions. Each time the system computed offset from automatic registration was noted and compared with the applied table offset.

2.6. *Image quality checks*

2.6.1. *MV planar Imaging*

Spatial resolution and contrast-to-noise ratio: The spatial resolution and the contrast to noise ratio of the planar MV images were evaluated by acquiring the planar image of QC-3V phantom, placed on the surface of the imager at SID 130 cm. The obtained images were evaluated automatically using the portal image processing programme to calculate the spatial resolution and the contrast-to-noise ratio. The obtained values were compared to the baseline values measured during commissioning.

2.6.2. *MV CBCT imaging*

The image quality phantom, shown in Fig. 2 was used to assess the image quality of CBCT image, such as uniformity, noise, spatial resolution and contrast resolution. The phantom was aligned with the machine isocentre using the lines engraved on the phantom, X-RETIC and room lasers. MV CBCT images were acquired to encompass the entire phantom, with 15 MU (monitor unit) acquisition protocol and reconstructed with 1 mm slice thickness, 1 mm^2 pixel size and smoothing head and neck filter.

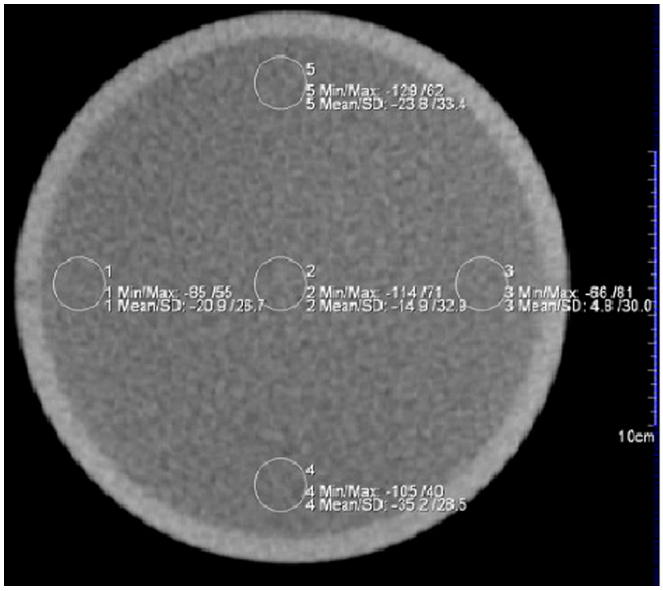

Fig. 3 – Five ROIs marked on central slice in section 1 of the image quality phantom to measure uniformity and noise. The means and standard deviations in pixel values of the five ROIs were within our specifications.

Uniformity and noise: The uniform solid water, section 1 of the image quality phantom was used to evaluate image noise and uniformity. On the CBCT image of this section, five circular regions of interest (ROIs) were drawn; one in the centre and four in the periphery at 12, 3, 6, and 9 o'clock positions, as shown in Fig. 3. For each of the 5 ROIs, the mean and the standard deviation of the pixel values were used to determine the image uniformity and noise in the CBCT image, respectively. The images were visually checked for artefacts. The obtained results were compared against baseline results.

Contrast resolution for CBCT: The image quality phantom's low and high contrast sections 2 and 4 have inserts of 8 different density material embedded on solid water background SIG (standard imaging grade). Each material has six inserts of circular dimensions of diameter 20, 10, 7, 5 and 3 mm. The relative electron density of each material with respect to the background is known, given in Table 2. On the acquired CBCT images, the number of inserts visible for each material was noted by adjusting the window and width of the image for better visualisation. These were compared with the baseline values.

Spatial resolution for CBCT: The spatial resolution section 3 of the image quality phantom consists of 11 bar groups with different resolution and five bars in each group. The dimensions of bars in each group are given in Table 3. On the CBCT image of this section, the number of bar groups in which all the bars are visible were counted and compared with the baseline.

2.6.3. *Imaging dose*

The portal imaging low dose rate output and cone beam output were checked monthly as part of routine output calibration. The beam output was calibrated routinely to deliver 1 cGy/MU with ±2% accuracy. The imaging dose from clinically used imaging protocols in MV planar and CBCT imaging was

Table 2 – Characteristics of insert materials in sections 2 and 4 of the image quality phantom.

Phantom section	Material	Physical density (g/cc)	Electron density relative to background	No. of inserts visible	Size of smallest visible insert (mm)
2	SIG – background	1.02	1	–	–
2	1% SIG	1.03	1.01	1	20
2	3% SIG	1.05	1.03	1	20
2	Brain	1.05	1.05	3	7
2	Liver	1.09	1.07	4	5
4	SIG – background	1.02	1	-	-
4	Inner bone	1.14	1.09	4	5
4	Acrylic	1.18	1.17	4	5
4	Bone – 50% $CaCO_3$	1.56	1.48	5	3
4	Air	0.0012	0.001	5	3

Table 3 – Bar group properties in section 3 of the image quality phantom Imaging dose.

Visible no. of bar groups	Width (mm)	Height (mm)	Corresponding spatial resolution (lp/mm)
1	7.5	12.0	0.067
2	5.0	12.0	0.1
3	3.3	12.0	0.15
4	2.5	12.0	0.2
5	2.0	12.0	0.25
6	1.67	12.0	0.3
7	1.25	12.0	0.4
8	1.0	10.0	0.5
9	0.83	6.6	0.6
10	0.62	5.0	0.8
11	0.50	4.5	1

evaluated annually, using a 0.6cc farmer ionisation chamber placed in the centre of a solid water phantom of dimensions $30 \times 30 \times 30\,cm^3$, with the chamber positioned at the treatment isocentre. A pair of orthogonal MV images was acquired with 2 MUs for each image and dose from each set-up verification image was measured. MV cone beam images were acquired with 6, 8 and 15 MU protocols and the accumulated dose for each protocol was measured.

3. Results

3.1. *Safety interlock checks*

The collision and safety interlocks were checked and verified daily and were found to be functional. All the mechanical movements of the machine were restricted with the motion stop interlock activated. The door interlock was functional when interrupted during imaging.

3.2. *Mechanical and geometric tests*

Imager positioning/repositioning: The positioning accuracy of the imager was measured with the variation between the expected and measured distances of the five markers from the isocentre. The repositioning accuracy was measured with the variations in the markers positions between the two images acquired before and after repositioning. The results were averaged for 3 years and presented in Table 4. It can be observed that the imager positioning accuracy and reproducibility was within ±1 mm.

Imaging and treatment co-ordinate coincidence: Fig. 4 shows that the misalignment of the MV planar image centre with the treatment beam isocentre was less than ±1 mm. The mean and standard deviation of misalignment at gantry angle 0°, 90°, 180° and 270° were 0.49 ± 0.14 mm, 0.57 ± 0.16 mm, 0.46 ± 0.16 mm and 0.54 ± 0.14 mm, respectively for a period of 3 years.

Image scaling: This test was performed monthly for 3 years by imaging the radio-opaque markers at known distances from each other, at different SIDs between 115 and 160 cm. The mean variation between the measured and actual distance was 0.5 ± 0.6 mm, over a period of 3 years.

Mechanical alignment through full range of imager travel: Fig. 5 shows that the flat panel mechanical misalignment was within 1 mm along any direction over a period of 3 years.

Geometric accuracy: Fig. 6 shows the variation between the expected and observed position of the beads. In all the three directions the results were within the tolerance of ±2 mm throughout the 3 year period.

Table 4 – Results showing the positioning/repositioning accuracy of the imager.

Marker	Mean variation ± standard deviation (mm)	
	Positioning accuracy	Repositioning accuracy
1	0.2 ± 0.3	0.0 ± 0.0
2	0.1 ± 0.7	0.0 ± 0.1
3	0.2 ± 0.7	0.1 ± 0.1
4	0.4 ± 0.5	0.1 ± 0.1
5	0.1 ± 0.4	0.0 ± 0.1

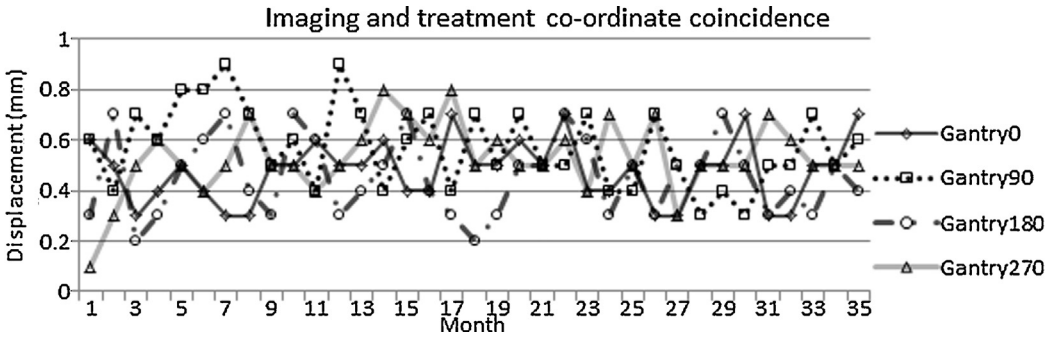

Fig. 4 – Results of monthly measurements of imaging and treatment co-ordinate coincidence over a period of 3 years.

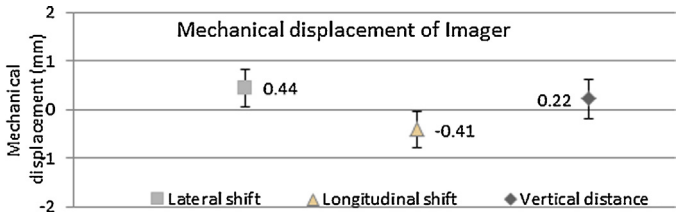

Fig. 5 – Mean mechanical displacement of the imager at different SID over a period of 3 years.

Image registration and offset calculation accuracy: It was found that the system computed off-set were well within ±2 mm of applied off-sets in any direction. It was found that if the two datasets were more than 4 cm apart, automatic registration failed to align the images successfully. It was required to manually move the planning image in closer alignment with the treatment image and perform the automatic registration.

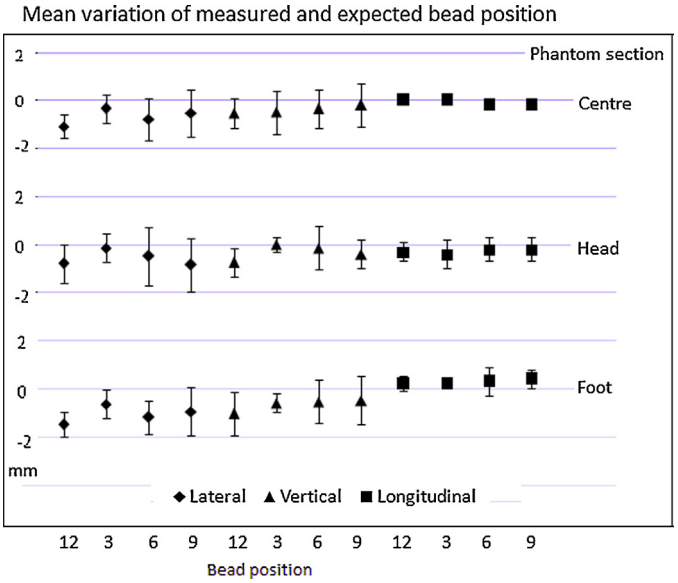

Fig. 6 – Results of mean variation in the bead positions in lateral, longitudinal and vertical direction.

3.3. *Image quality tests*

3.3.1. *MV planar imaging – spatial resolution and contrast-to-noise ratio*

Fig. 7 shows the MV planar image of the QC-3V phantom. From the image, spatial resolution and contrast to noise ratio were automatically evaluated using the portal image processing programme. The contrast-to-noise ratio on the planar images varied within ±2% of baseline, with the mean measured value 797.77 ± 7.43. The spatial resolution was defined using the f50 (frequency at 50% relative modulation transfer function) value in units of line pairs/mm. The mean of measured value was 0.432 ± 0.02 lp/mm, within 4% of the baseline.

3.3.2. *MV CBCT imaging*

Uniformity and noise: The baseline and measured mean and standard deviation of the pixel values were tabulated in

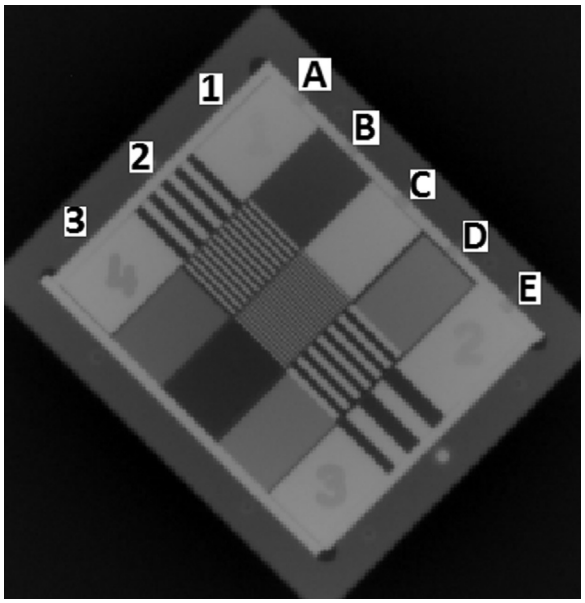

Fig. 7 – MV planar image of QC-3V phantom. Elements 1B (15 mm Al), 1C (15 mm Pb), 1D (7.5 mm Pb; 7.5 mm PVC), 3B (5 mm Pb; 10 mm PVC), 3C (15 mm PVC) and 3D (7.5 mm Pb; 7.5 mm PVC) were used for CNR calculation; 2A (0.20 lp/mm), 2B (0.40 lp/mm), 2C (0.75 lp/mm), 2D (0.25 lp/mm) and 2E (0.10 lp/mm) were used to calculate spatial resolution.

Table 5 – Results of uniformity and noise measurements for MV CBCT image.

ROI	Acceptable range	Baseline	Measured[a]
Mean ROI_{centre}	(−30, +42)	−15.9	−13.5 ± 1.2
SD ROI_{centre}	(−30, +42)	34.2	32.6 ± 2.7
Mean $ROI_{periphery(9\ o'clock)} - ROI_{centre}$	(−80, +80)	10.2	10.9 ± 1.4
Mean $ROI_{periphery(3\ o'clock)} - ROI_{centre}$	(−80, +80)	6.5	5.4 ± 1.5
Mean $ROI_{periphery(6\ o'clock)} - ROI_{centre}$	(−80, +80)	26.7	25.4 ± 2.8
Mean $ROI_{periphery(12\ o'clock)} - ROI_{centre}$	(−80, +80)	−14.2	−13.9 ± 2.4

[a] Mean ± standard deviation of measured value for the 3 years period.

Table 5. The results show that the measured values are well within the acceptable range specified by the manufacturer. Also there was no visual evidence of artefacts in the image.

Contrast resolution: Fig. 8 shows the low and high contrast section 2 and 4 axial CBCT images of image quality phantom. The contrast resolution of the MV CBCT images were measured monthly and the visible number of inserts agreed with the baseline throughout the period of 3 years. The number of inserts visible and the material densities are tabulated in Table 2. For the clinically used 6, 8 and 15 MU imaging protocols, the objects of size less than 2 cm with contrast 1% and 3% of background were not visible.

Spatial resolution: Spatial resolution was checked monthly by counting the number of visible bar groups in the CBCT image of the phantom section 3, as shown in Fig. 9. Six bar groups were completely visible, which corresponds to spatial resolution of 0.3 lp/mm (line pairs per mm), as given in Table 3 and these results were found to match the baseline. Generally, the spatial resolution can be increased by decreasing the pixel size, but at the cost of increased image reconstruction time.

3.3.3. *Imaging dose*

The MV planar dose measurements were performed annually and compared with the baseline values. The dose accumulated at the isocentre from the orthogonal MV images was within 3% of the baseline throughout the 3 year period. For MV CBCT dose measurements, the dose at the isocentre was within 3% of the baseline throughout the 3 year period. The mean of the dose measured for the 3 years is tabulated in Table 6.

4. Discussion

In this study, we share our three years' experience in the development and implementation of a quality assurance programme of the MV image guidance system on Siemens Oncor Expression linear accelerator. The QA tests include the system safety, mechanical and geometrical accuracy, image quality and dose performed for the MV planar and CBCT system. The tests were performed using the QA equipment supplied by the manufacturer along with the image guidance system and using simple methods developed in-house, such that the tests can be performed without further cost for QA equipment. Initially the tests were performed more frequently than specified by the manufacturer to ensure stable characteristics of the imaging system. The data collected from the QA tests in the initial year were used as the basis for establishing the tolerance from the baseline value established during commissioning.

Table 6 – Imaging dose at isocentre for different imaging protocols.

Imaging protocol	Dose at isocentre (cGy)	
	Baseline	Mean ± SD of measured dose
6 MU protocol	5.05	5.03 ± 0.12
8 MU protocol	6.14	6.10 ± 0.08
15 MU protocol	9.97	10.07 ± 0.15
Orthogonal MV planar – 2 MU each	2.99	2.98 ± 0.07

The system safety interlocks were checked daily for its functionality for safe clinical use. The Flat Panel imager requires daily initialisation before use. It was noted that on some occasions, the system gives collision interlock falsely, needs to be brought back to the home position manually and restart the initialisation. In such cases, additional care is required while performing daily mechanical tests to check for any misalignments.

Since the mechanical alignment of the imager with treatment beam is crucial for evaluating patient set-up errors, the mechanical checks are considered the most important among all tests. During installation of the imager, the machine service Engineers aligned the imager within ±1 mm accuracy and the residual errors were corrected using accurate positional calibration of imager and verified by the Physicist. The imager positional calibration data can be stored in any storage media and kept as a backup. The imager positioning test and imaging and isocentre co-ordinate coincidence test were performed daily for zero gantry angle and monthly for the other three cardinal gantry angles. Our results show excellent agreement, within ±1 mm with respect to the expected value. During one of our routine image alignment checks, we found that the image was misaligned by a small angle of around 0.3° while the imaging centre matched with the treatment isocentre. When the imager protective cover was removed to check the physical alignment, we noticed that the imager was rotated by a small angle and was then corrected. Special care should be taken when working near the imager to avoid any object falling on the imager accidentally.

The MV CBCT image quality is poorer than the conventional kV (kilo voltage) beam image quality, but sufficient to successfully perform automatic image registration within 2 mm accuracy and help visualise soft tissues and bony structures for the set-up verification and anatomy changes around the tumour.[12] Poor image quality is not intrinsically responsible for errors in patient positioning, but may

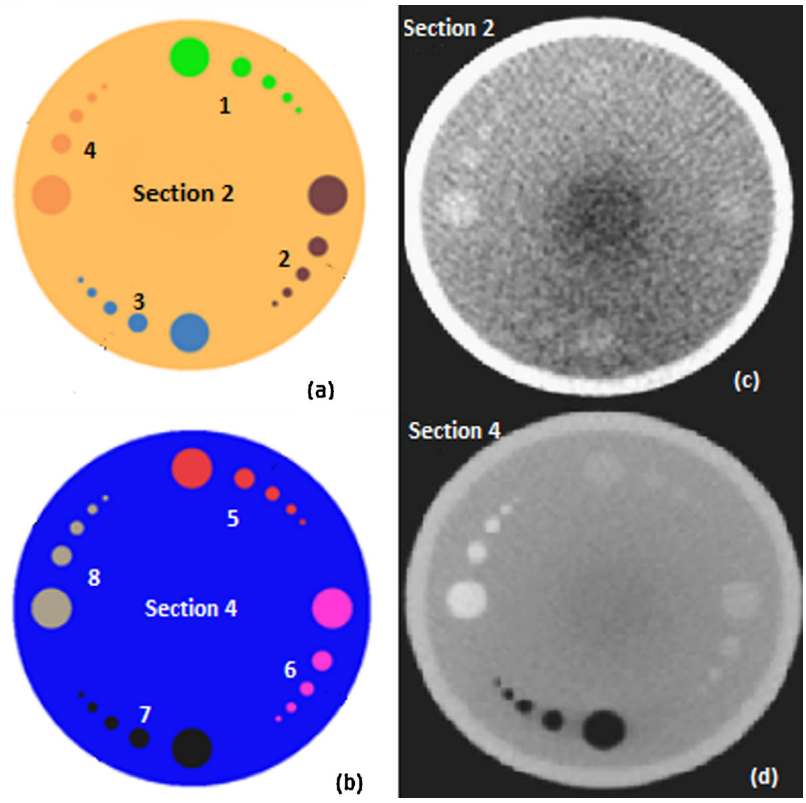

Fig. 8 – (a) Low contrast section 2, (b) high contrast section 4 of the image quality phantom. Each section has inserts of four different materials: (1) 1% SIG, (2) 3% SIG, (3) brain, (4) liver, (5) inner bone, (6) acrylic, (7) air and (8) CB2 (bone – 50% $CaCO_3$). These material characteristics are given in Table 2. (c) MV CBCT image of section 2 and (d) MV CBCT image of section 4 of image quality phantom, acquired with 15 MU imaging protocol.

cause misalignments during the image registration between planning and cone beam CT data set in the soft tissue region.

For optimal image quality performance, the MV system requires periodic 2D gain calibration, cone beam geometric calibration and dead pixel map correction. We perform these calibrations every four weeks as recommended by the manufacturer. It is also important to perform these calibration procedures and QA tests after major repairs of the imaging system.

We used 15 MU protocol on image quality phantom for testing the image quality of MV CBCT images. There was no much noticeable difference in the image quality in the low MU (6 or 8 MU) protocols. This is because of smaller phantom size used for our tests. Imaging pelvic region requires more MUs than imaging the head and neck for good image quality because of

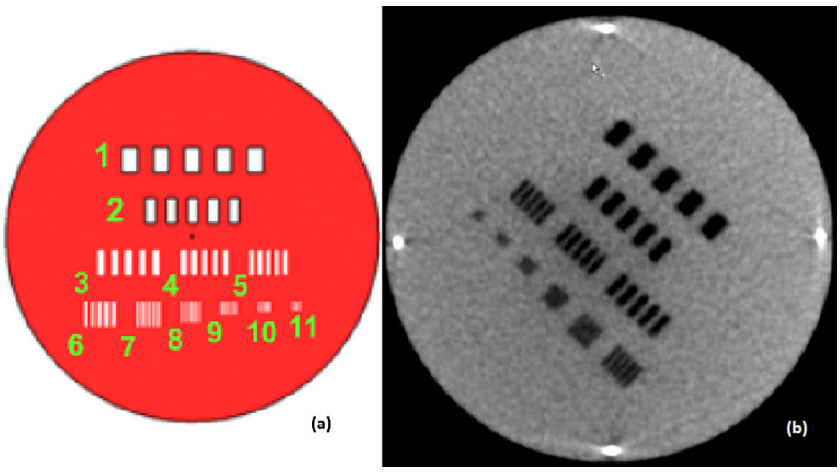

Fig. 9 – (a) Spatial resolution section 3 of the image quality phantom. Eleven bar groups with different numbers of line pairs per millimetre are inserted in this section. (b) MV CBCT image of section 3, acquired with a 15 MU protocol.

the variation in off-axis response of the imager detectors.[13] For a good quality image, we require higher MU protocol, which increases patient dose. It is possible to incorporate the patient dose into treatment plan to eliminate the extra dose used for high quality image guidance.[14,15] Since we did not intend to use the CBCT images for dose calculation in treatment planning, we did not perform HU CT calibration for CBCT images as part of the quality assurance programme. We suggest performing HU calibration monthly to use the CBCT images for dose calculation.

The low dose rate 50 MU/min output and cone beam output, which are used for image acquisition, were calibrated monthly to deliver 1 cGy/MU, for $10 \times 10\,cm^2$ field size at depth of maximum dose. The planar and CBCT imaging dose at the isocentre, measured annually with ionisation chamber at the centre of the $30 \times 30 \times 30\,cm^3$ slab phantom were within 3% of baseline dose values. We measure this to check the consistency in the dose delivered during imaging. In our QA tests we did not intend to measure the dose for patient in each imaging protocol. The QA programme can be improved by measuring patient imaging dose for specific sites such as the head & neck and pelvis, in anthropomorphic phantom using ionisation chambers, radiochromic films or TLDs.[16]

There are several clinical applications with the use of image guidance system. Few examples are: (i) it provides image guidance to determine the target position with respect to treatment beam[17,18]; (ii) it is used to estimate the patient positioning uncertainties and to justify the CTV-PTV margin for different sites[19]; (iii) it is used in dose calculation[20] and exit dosimetry to predict the dose delivered to the patient in each fraction[21]; (iv) it is used to investigate the changes in the tumour volume and thereby determine the requirement for adaptive planning[22]; (v) it provides 3D anatomic information without artefacts for patients with implanted metallic objects.[23]

The periodic calibration and QA of imaging system gives confidence to apply IGRT clinically.

5. Conclusion

The MV imaging system provides 2D planar and 3D volumetric cone beam images for radiotherapy patient treatment setup verification and inter-fractional anatomy changes in the patient treatment course. In this study, we have developed and implemented the quality assurance programme for the image guidance system. We have studied the safety, geometric precision and image quality to use the system clinically. We conclude that the MV image guidance system performance is adequately accurate to perform IGRT and insist to perform periodic quality assurance tests and calibration for the system.

Conflict of interest

None declared.

Financial disclosure

None declared.

REFERENCES

1. Morin O, Gillis A, Chen J, et al. Megavoltage cone-beam CT: system description and clinical applications. *Med Dosim* 2006;**31**:51–61.
2. Jaffray DA, Siewerdsen JH, Wong JW, Martinez AA. Flat-panel cone-beam computed tomography for image-guided radiation therapy. *Int J Radiat Oncol Biol Phys* 2002;**53**:1337–49.
3. Lee C, Langen KM, Lu W, et al. Assessment of parotid gland dose changes during head and neck cancer radiotherapy using daily megavoltage computed tomography and deformable image registration. *Int J Radiat Oncol Biol Phys* 2008;**71**:1563–71.
4. Bylund KC, Bayouth JE, Smith MC, et al. Analysis of interfraction prostate motion using megavoltage cone beam CT. *Int J Radiat Oncol Biol Phys* 2008;**72**:949–56.
5. Klein EE, Hanley J, Bayouth J, et al. Quality assurance of medical accelerators: report of AAPM Radiation Therapy Committee Task Group 142. *Med Phys* 2009;**36**:4197–212.
6. Bissonnette J-P. Quality assurance of image-guidance technologies. *Semin Radiat Oncol* 2007;**17**:278–86.
7. Herman MG, Balter JM, Jaffray DA, et al. Clinical use of electronic portal imaging: report of AAPM Radiation Therapy Committee Task Group 58. *Med Phys* 2001;**28**:712–37.
8. MVision Physicist self-led training. Siemens Medical solutions, Inc.: Concord, CA.
9. Pouliot J, Bani-Hashemi A, Chen J, et al. Low-dose megavoltage cone-beam CT for radiation therapy. *Int J Radiat Oncol Biol Phys* 2005;**61**:552–60.
10. Olivier G, Moyed M. Commissioning and clinical implementation of a mega-voltage cone beam CT system for treatment localization. *Med Phys* 2007;**34**:3183–92.
11. Abou-elenein HS, Attalla EM, Ammar H, et al. Megavoltage cone beam computed tomography: commissioning and evaluation of patient dose. *J Med Phys* 2011;**36**:205–12.
12. Dąbrowska SZ, Kukołowicz PF, Szebek PC, et al. Comparison of image registration performed with MV cone beam CT and CT on rails and Syngo TM Adaptive Targeting software. *Rep Pract Oncol Radiother* 2009;**14**:122–32.
13. Morin O, Aubry JF, Aubin M, et al. Physical performance and image optimization of megavoltage cone-beam CT. *Med Phys* 2009;**36**:1421–32.
14. Morin O, Gillis A, Descovich M, et al. Patient dose considerations for routine megavoltage cone-beam CT imaging. *Med Phys* 2007;**35**:1819–27.
15. Miften M, Gayou O, Reitz B, et al. IMRT planning and delivery incorporating daily dose from mega-voltage cone-beam computed tomography imaging. *Med Phys* 2007;**34**:3760–7.
16. Gayou O, Parda DS, Johnson M, et al. Patient dose and image quality from mega-voltage cone beam computed tomography imaging. *Med Phys* 2007;**34**:499–506.
17. Packard M, Kirichenko A, Gayou O, et al. Use of implanted gold fiducial markers with MV-CBCT image guided IMRT for pancreatic tumors. *Pract Radiat Oncol* 2013;**3**:S14–5.
18. Paluska P, Hanus J, Sefrova J, et al. Utilization of cone-beam CT for offline evaluation of target volume coverage during prostate image-guided radiotherapy based on bony anatomy alignment. *Rep Pract Oncol Radiother* 2012;**17**:134–40.
19. Juan-Senabre XJ, López-Tarjuelo J, Conde-Moreno A, et al. Uncertainties and CTV to PTV margins quantitative assessment using cone-beam CT technique in clinical application for prostate, and head and neck irradiation tumours. *Clin Transl Oncol* 2011;**13**:819–25.
20. Morin O, Chen J, Aubin M, et al. Dose calculation using megavoltage cone-beam CT. *Int J Radiat Oncol Biol Phys* 2007;**67**:1201–10.

21. Chen J, Morin O, Aubin M, et al. Dose-guided radiation therapy using megavoltage cone-beam CT. *Br J Radiol* 2006;**79**:S87–98.
22. Foroudi F, Wong J, Haworth A, et al. Offline adaptive radiotherpy for bladder cancer using cone beam computed tomography. *J Med Imag Radiat Oncol* 2009;**53**:226–33.
23. Hansen EK, Larson DA, Aubin M, et al. Image-guided radiotherapy using mega-voltage cone-beam computed tomography for treatment of paraspinous tumors in the presence of orthopedic hardware. *Int J Radiat Oncol Biol Phys* 2006;**66**:323–6.